Calibration of GHRS Burst Noise Rejection Techniques

E. A. Beaver[1], R. D. Cohen[1], A. Diplas[1], H. Garner[2], S. R. Heap[3]
M. Loveland[1] and R. D. Robinson[4]

Abstract

For observing very faint objects with the GHRS, the limiting magnitude is not only set by the instrumental sensitivity but by detector dark-noise. The measured average dark level for the D2 detector is 0.01 counts/sec/diode, the GHRS dark specification; almost all of the dark appears to be due to space radiation particle noise. We report here our calibration of the D2 burst noise rejection algorithm with the Proposal 4012 data set. For a FLYLIM setting of 1, where a frame sum of 2 counts or more is rejected, we find the average dark level reduced some 80 percent to 0.002 counts/sec/diode for 0.2 second frame times. In addition we have developed a signal-to-noise code that determines the optimum FLYLIM setting for a specific object signal level.

I. Introduction

Radiometric tests of the GHRS instrument during Science Verification have shown that the GHRS is a very sensitive instrument. For observing faint objects, e.g. high-z quasars, the limiting factor is not so much sensitivity but detector dark-noise. The measured dark-noise on the GHRS detectors is due to space particle radiation. If we are to make use of this sensitive instrument on very faint objects, we must take all possible steps to lower the dark-noise level. In order to calibrate the GHRS burst noise rejection algorithms, Proposal 4012 was developed, entitled DARK-COUNT STATISTICS FOR GHRS DETECTOR D2. Proposal 4012 is designed to find out about how many times the diode array registers a 1 count, how many times 2 counts, etc. in the GHRS frametime. We report here our analysis of the data from Proposal 4012.

During extensive ground test activity, the GHRS detectors registered about 2×10^{-4} counts/sec/diode dark-count level at high voltage. However in the near-Earth orbit of the *HST*, the radiation environment elevates the Digicon detector dark-count level. The GHRS team has carried out extensive measurements of the particle radiation via Proposals 1407 and 1408 during science verification. These tests have served to describe the dark-counts as a function of *HST* position (latitude, longitude) and to give a dark-count rate for the D2 detector outside the SAA, varying from 0.007 counts/sec/diode at 0 degrees geomagnetic latitude to about 0.014 counts/sec/diode at

1. CASS, University of California, San Diego, La Jolla, CA 92093-0111
2. Ball Aerospace Systems Group, PO Box 1062, AR-1, Boulder, CO 80306
3. Goddard Space Flight Center, Code 681, Greenbelt, MD 20771
4. CSC, Goddard Space Flight Center, Code 681/CSC, Greenbelt, MD 20771

40 degrees geomagnetic latitude. For a long, multi-orbit observation, the GHRS dark-count averages out to about 0.01 counts/sec/diode, which is the original GHRS specification established at contract award in 1978; we are attempting to improve the GHRS limiting magnitude performance beyond specification.

Monte Carlo modeling of the GHRS detector dark-noise indicates that the predominant source of orbital noise comes from Cerenkov light flashes generated by cosmic rays transiting the Digicon faceplate (Beaver et al. 1991). The character of this noise is seen to be the essentially instantaneous formation of single counts on many diodes from individual cosmic ray induced light flashes in the faceplate (Rosenblatt et al. 1991). The Monte Carlo Cerenkov Model calculations further predict that the distribution of particle background events is very different from that of the Poisson distributed starlight and suggest a significant reduction in detector background will occur by the use of a rejection algorithm that is designed to take advantage of this difference. The GHRS rejection algorithm simply sums the number of counts in a frame of data and rejects the frame from the exposure sum if the sum is greater than a preset limit parameter. For faint objects and short frame times, most of the Poisson distributed signal frame sums are zeros or ones whereas a large percentage of the exponential-like distributed dark frame sums are greater than one.

Science Verification tests have also been done to see to what extent the dark-count rate could be lowered through use of the GHRS high speed (burst rejection in 10 microseconds) burst noise rejection circuit with the result that it reduces the dark-count rates by only 20 or so. The problem is that the counter can only detect bursts of particle radiation on the order of 8 or more photo-electrons, whereas the particle hit patterns generally come in smaller packets.

This possibility was not unexpected, and the flight software accordingly has means of rejecting data obtained in the ACCUM mode by comparing the sum of the counts on the diode array with the user-set threshold, FLYLIM, and discarding frames with sums greater than FLYLIM from the accumulation. This noise rejection technique was standard fare on the ground-based Digicons (Beaver et al. 1976), and so it was transferred to the GHRS flight software. In fact, the reason why we have a 200-ms frametime instead of 50-ms, as we initially wished, is to allow time for the NSSC-1 to do this frame-rejection.

The first astronomical use of the GHRS burst noise rejection technique occurred with observations of the star AU Mic (Woodgate et al. 1992 and Maran et al. 1993) where the authors searched the spectra for indications of flaring activity. These observers of AU Mic used the GHRS in the rapid readout mode at 0.4 seconds per frame with each frame sent to the on-board tape recorder. They applied burst noise rejection techniques on the data post-facto.

II. Proposal #4012 Data

The dark-noise statistics proposal, #4012, was run in two parts. The first part was run on Side 2 in Oct 1992 and is composed of 6 *HST* orbits of rapid readout data with 0.35 second per readout frame. Only the first four orbits are analyzed here, since the last two orbits penetrated the SAA. Ideally we would have liked to monitor the

background by sending down frames every 200-ms and analyzing them. This data rate would require the 1-Mhz link, which is not available for long periods of time. Instead the dark was monitored every 350 ms, sending each frame of data to the tape recorder.

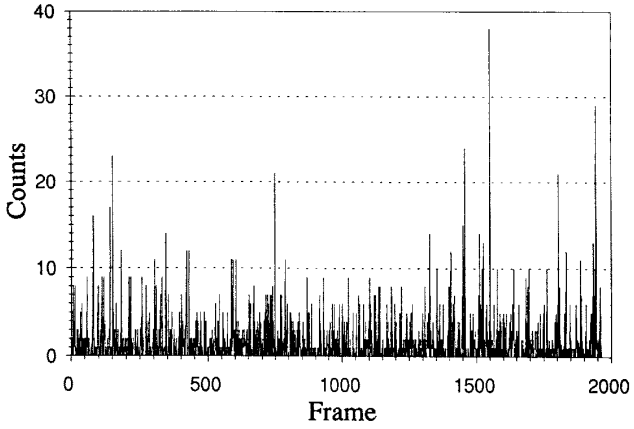

Figure 1: H5611 Frame Sums

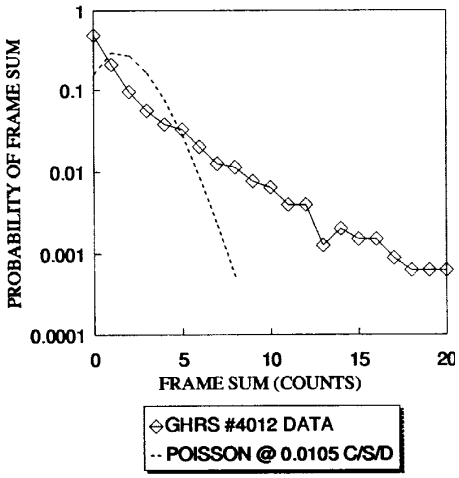

Figure 2: #4012 Dark Event and Poisson Distribution

Analysis of the 7864 frames of dark data gives the frequency distribution of the frame sums and allows prediction of SIGNAL/NOISE ratios for faint objects. The four orbits of data are located at entry numbers 5611 to 5616 in the GHRSLOG. This observation is strictly internal dark-count. The carrousel is at the safe position and the shutter is closed. No external light should reach the detector.

During this observation five diodes were turned off; they are diodes 110, 150, 279, 348, and 448, numbered starting from 1. Thus 495 science diodes are active. The frame sums for the first orbit (H5611) are displayed in figure 1. The distribution of frame sums for the entire data set is shown in figure 2, along with a distribution that would be expected from a Poisson distribution of frame sums at the 0.35 second framing rate and average dark rate. If the dark-count were due to photocathode thermionic emission, for example, it would be Poisson distributed. Clearly the distribution of frame sums for GHRS orbital dark-noise is non-Poisson in character. The largest frame sum in the data set is 138 counts!

The average size of a non-zero frame sum is 3.5 counts. The average dark-count integrated over the four orbits is 0.01057(±0.00008) counts/sec/diode. Note that this small formal error is due to good counting statistics; another dark observation exposed over a different orbital track than 4012 could have a somewhat higher or lower average dark than the quoted 4012 dark level. Although a long exposure tends to average down the factor of 2 geomagnetic latitude variation in the dark rates, some smaller differences remain in the dark level for different orbit tracks.

Table 1: #4012 Frame Distribution

Frame Sum (Counts)	Fraction of Frames with Frame Sum	Fraction of Frames < Frame Sum	Fraction of Dark Counts < Frame Sum
0	0.49	0	0
1	0.21	0.49	0
2	0.096	0.70	0.12
3	0.056	0.79	0.23
4	0.038	0.85	0.33
5	0.032	0.89	0.42
8	0.011	0.95	0.64
10	0.00065	0.97	0.73

Statistical information from the experiment is listed in Table 1. Figure 3 shows the dark-count sum from this observation along with the dark-count sum with a frame sum rejection set at two or greater. As seen from Table 1, 49 percent of the 7864, 0.35 second frames have no dark-counts. For a setting of FLYLIM=1, the lowest meaningful setting, 70 percent of the frames are accepted; however the dark-count is

FIGURE 3: #4012 DARK-COUNT FOR FRAME SUM >1 REJECTION AND WITHOUT REJECTION

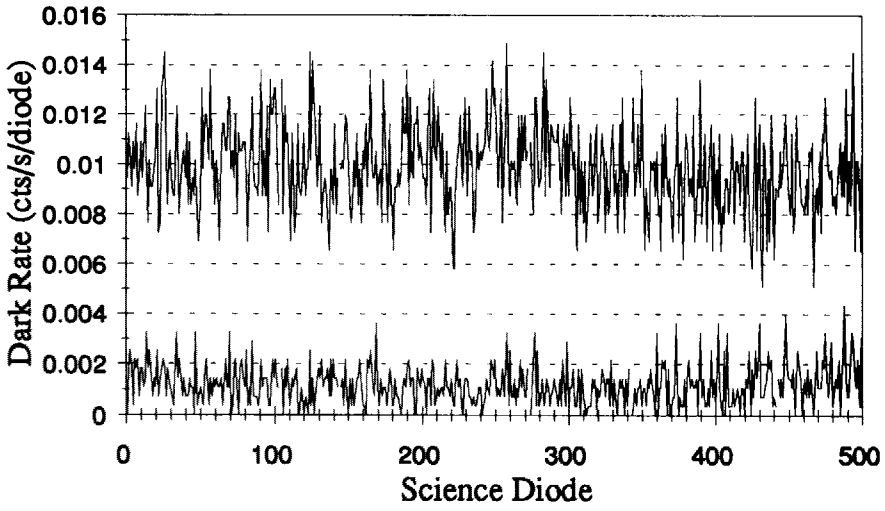

reduced to 12 percent of the full non-rejection value. As will be demonstrated in section 3, for FLYLIM=1, the fraction of time available for signal collection is the fraction of frames with no dark-counts. Thus for a faint object signal where 2 or more counts per frame is unlikely, we would expect the collected signal to be 49 percent of the full, non-rejection level for the 0.35 second frame time. Note, however, that the apparent count rate from the object will be lower than the rate without rejection

because additional time is spent counting single dark photons. Clearly a shorter frame time would be advantageous for better signal collection since the percentage of frames with no counts will increase with decreasing frame time. The second part of #4012, discussed next, addresses the need for faster framing by testing real time burst noise rejection at 0.2 seconds per frame.

The second section of GHRS Side 2 #4012 was run in February 1993. It is a dark observation of 7 bins with 215 patterns per sub-exposure; this observation has six sub-exposures and the frame time is 0.2 seconds. FLYLIM was set to 1, which means frames with 0 or 1 counts in the ON-THE-FLY-ADDER (OTFA) are accepted; those frames with 2 or more counts in the OTFA are rejected. This observation is entry number 6037 in the GHRSLOG database. Figure 4 shows the exposure sum for all frames. The specified exposure time for this observation is 1806 seconds. However, a study of the observation logs shows that frame rejection increased the exposure time by 24.3 percent to 2245.4 sec. In other words, out of a total of 11227 frames, 2197 frames were rejected. To be consistent, we use this larger exposure time to calculate an average dark rate of 0.00207(±0.00004) counts/sec/diode for this FLYLIM=1 dark observation at 0.2 second frame time. The reduction in dark rate with FLYLIM=1 is certainly dramatic and on the order of 80. Successful operation of this observation shows that the flight software for a typical science observation with FLYLIM enabled works fine.

FIGURE 4: #4012, PART 2 DARK WITH FLYLIM=1 AT 0.2 SEC. FRAME

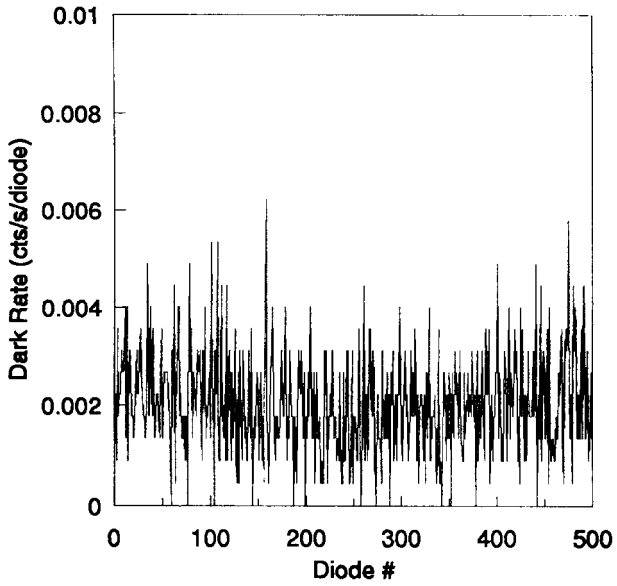

Table 2: Science-to-Dark Ratios

FLYLIM (counts)	Frame Time (sec)	Bkgd/Science (B/d)	Statistical Error (±)
1	0.20	12.2461	0.850
1	0.35	16.259	1.177
2	0.35	11.418	0.700
3	0.35	9.572	0.533
4	0.35	8.468	0.444
9	0.35	6.4848	0.293
19	0.35	5.6161	0.245
∞	all	5.384	0.121

Additional information concerning the dark level comes from the large background diodes; proposal #4012 calibrates the response of the background diode dark sensitivity relative to the science diode dark sensitivity. At each end of the 500 diode science array are located two background diodes, situated above and below the axis of the science diodes. Each of the background diodes has geometrically 5 times the collection area of an individual science diode. In Table 2 we list the Background-to-Science Diode ratios (B/d) determined from our analysis, where

$$\frac{B}{d} = \left(\frac{\text{sum of 4 bkgd diodes}}{4}\right) \Big/ \left(\frac{\text{sum science diodes}}{495}\right) \tag{1}$$

Note that this ratio is a strong function of the FLYLIM setting and frame time. Of course our only calibration of B/d at 0.2 second frame time is at the FLYLIM setting of one.

Also as part of this effort we have analyzed all previous (up to 9/93) Proposal 1408 dark observations in order to find the best possible value for the normal B/d. This “no burst noise rejection” result is B/d = 5.384 ±0.121 and represents some 140 minutes of dark observation time. The statistical uncertainty of 0.121 in B/d is larger than we would prefer since it alone can lead to an uncertainty in the science observation dark level equivalent to the faint signal level under investigation. Hopefully considerably more dark observations can be taken to improve the accuracy of B/d.

III. GHRS Frame Rejection Signal to Noise Calculations

In the simplest case the signal to noise relationship for photon counting statistics is given by the equation in the GHRS Handbook:

$$(S/N)^2 = \left[\left(\frac{s}{d}\right) \Big/ \left(\frac{s}{d+1}\right)\right] st \tag{2}$$

where s = object signal count rate, d = detector dark-count rate, and t = accumulation time for the observation. The dark event distribution statistics of Table 1 show that the dark-count rate can be significantly reduced and consequently S/N improved by rejecting frame sums above a preset limit; however, somewhat negating this S/N improvement is the loss of observation time and object signal caused by the rejection process. To accurately take these losses and gains into account and estimate the S/N improvement with frame rejection, we have developed a software S/N model based on the Table 1 results.

FIGURE 5: S/N CODE DISTRIBUTIONS FOR NO, 0.2, & 0.35 SEC. FRAMING

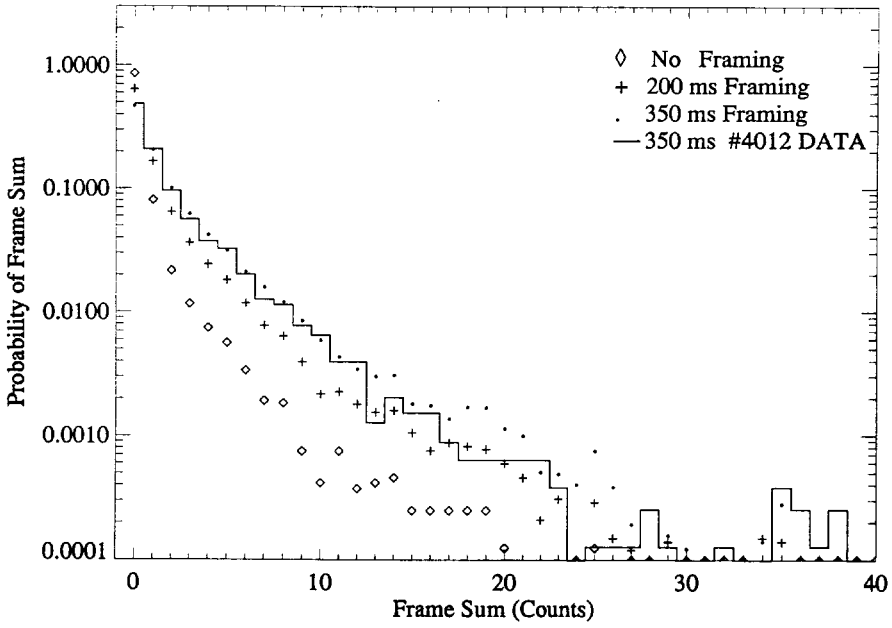

This S/N software model builds up two separate random number arrays, one for the dark frame count sums and the other for signal frame count sums. The object signal frame vector is easily filled by calls to the standard Poisson random number generator (Press et al. 1992). However, filling the dark-count array with random numbers distributed according to the Table 1, required programing a special random function, developed according to the "rejection method" (Press et al. 1992).

Since we also want to determine S/N improvement for other frame times than the 0.35 second framing, we have added a cosmic ray flux section to this S/N code. That is, the Table 1 distribution will change shape with frame time due to the different average number of cosmic ray induced Cerenkov events for a different frame time interval. We assume that the cosmic ray flux incident on the Digicon faceplate is Poisson distributed.

The S/N program flow is as follows: 1. The observation time, frame time, object signal level and detector dark level are entered into the program. 2. A frame loop is started to fill the dark and signal arrays. 3. For the frame number under consideration, a call is made to the cosmic ray Poisson random number generator to find the number of cosmic rays that transited the faceplate during the frame time. A call is then made

to the dark random number generator for each of these cosmic rays and the dark-count results are summed into the dark frame under consideration. 4. For the frame number under consideration, a call is made to the signal Poisson random number generator and the random signal result is placed in the signal frame under consideration. 5. The frame loop continues until the end of the observation time. 6. For each frame sum rejection level (FLYLIM), the Dark and Signal arrays are used to determine S/N from equation 2. 7. The optimum frame sum rejection level which maximizes S/N is determined.

Figure 5 shows the dark distributions determined from this S/N program for various frame times at the dark rate of 0.01 counts/sec/diode and an observation time of 20000 sec. Note in figure 5 the close approximation of the 0.35 second dark random number distribution to the actual distribution. However our S/N results for other frame times will be model dependent. The "no framing" distribution of Figure 5 is the distribution used in the dark random number generator and is constructed such that when used in the S/N Program with 0.35 second frame time, the observation 4012 frame distribution of Table 1 results.

As determined from our S/N code, Table 3 gives the optimum settings for FLYLIM for various object signal levels and frame times at a dark rate of 0.01counts/sec/diode. The fourth column, labeled "improvement," is given by $(s/n)^2/(S/N)^2$ where s/n and S/N are the signal to noise with and without burst noise rejection, at the indicated FLYLIM setting. This improvement number indicates the factor by which observation time is reduced to get the same S/N as that case with no burst noise rejection. For a frame time of 0.2 seconds and object signal of 0.001 counts/sec/diode, the exposure time is one half that to obtain the same S/N without burst noise rejection. As the signal level increases to the dark rate the advantage of using burst noise rejection decreases. Note that decreasing the frame time also improves the S/N performance for burst noise rejection.

Maran et al. 1993 point out that the fraction of time available for signal measurement is the fraction of dark frames with no counts. Our S/N code gives the same result. For the very faint object signal of 0.0004 counts/sec/diode at 0.2 second framing, 64 percent of the signal is accepted, and is to be compared with 64 percent of the dark frames having no counts (see figure 5).

Table 3: Optimum FLYLIM Setting for Various Object Signal Levels at a Dark Rate of 0.01 counts/sec/diode

Object Signal "S" (c/s/d)	Frame Time (sec)	Optimum FLYLIM (Count)	Improvement $\frac{(s/n)^2}{(S/N)^2}$	Signal Accepted (s/S)	Dark Accepted (d/D)	Time Lost $(1-t)/T$
0.0004	0.20	1	2.40	0.64	0.15	0.19
	0.35	2	1.88	0.67	0.22	0.22
0.001	0.20	2	2.00	0.80	0.27	0.12
	0.35	2	1.65	0.65	0.20	0.24
0.002	0.20	2	1.75	0.78	0.25	0.13
	0.35	3	1.50	0.75	0.29	0.18
0.003	0.20	2	1.56	0.76	0.24	0.14
	0.35	4	1.35	0.81	0.37	0.14
0.005	0.20	3	1.38	0.83	0.33	0.11
	0.35	5	1.24	0.84	0.42	0.12
0.0075	0.20	4	1.26	0.88	0.40	0.084
	0.35	6	1.15	0.86	0.47	0.10
0.01	0.20	5	1.18	0.90	0.47	0.067
	0.35	8	1.11	0.91	0.58	0.068
0.02	0.20	8	1.07	0.95	0.62	0.037
	0.35	12	1.04	0.95	0.68	0.043

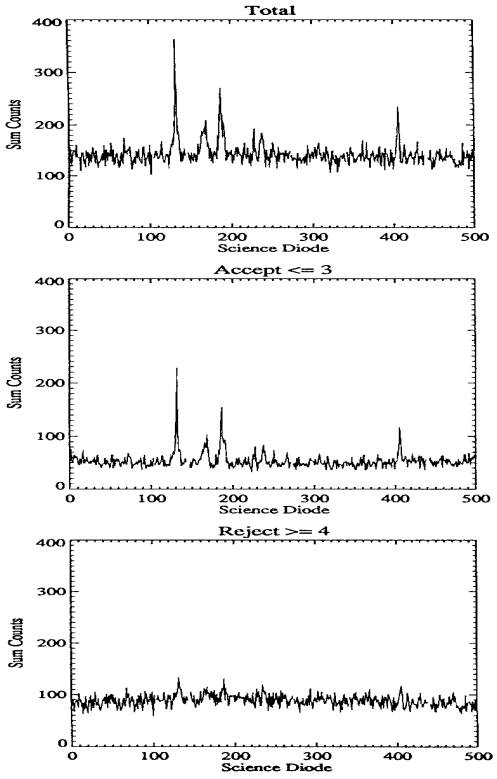

Figure 6: AU Mic star spectrum with optimal rejection.

IV. Rapid Readout Flare Star

As an example of the use of our results, we apply them to an existing (Maran et al. 1993) rapid readout data set for the star AU Mic, a star known for flare activity. This specific application is only meant to be used for illustration. The top plot in Figure 6 displays the GHRS G160M spectrum of AU Mic (without burst noise rejection) centered at about 1360Å. This rapid readout data set is composed of 31962 frames at 0.4 second per frame.

FIGURE 7: Comparison of AU Mic data with models at various signal levels:
s=0 cts/s/d, d=0.0111 cts/s/d
s=0.00095 cts/s/d, d=0.01015 cts/s/d
s=0.0021 cts/s/d, d=0.009 cts/s/d

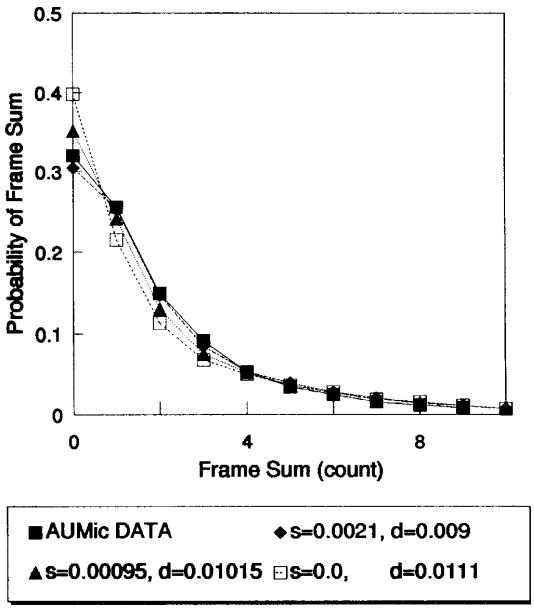

We use the Background-to-Science diode ratio (5.38 from Table 2) along with the AU Mic Background diode count from the observation to calculate a dark level of 0.01016±0.0012 counts/sec/diode as seen by the science diodes. Since the average total count as measured by the science diodes works out to be 0.01110 counts/sec/diode, the signal level works out to be 0.0009455±0.0012 counts/sec/diode. The large uncertainty in the Background-to-Science diode ratio has caused an uncertainty in the signal level greater than the actual signal level.

Another possible approach for determining the signal level in the data total is to compare the data distribution with model distributions generated by our S/N code for various percentages of signal and dark levels. The results of this approach are shown in figure 7. For the lower frame sum counts, the shape of the distribution is very sensitive to the signal and dark percentages. Note that before we would take this technique very seriously, we want to further investigate the stability of dark distribution data for different orbits and the degree of predictive accuracy of our S/N code.

However, for this illustrative work, we take the signal level to be ~0.002 counts/sec/diode, the best curve fit in figure 7; the dark level works out to be 0.0091 counts/sec/diode. Our S/N code gives the optimum FLYLIM=3 for these signal and dark level settings, where 73 percent of the signal is accepted and the dark is reduced to 28 percent of the normal level. The middle plot in figure 6 is the AU Mic spectrum for FLYLIM=3. We see a significant reduction in diode-to-diode variation and the possible presence of additional weak features in the AU Mic spectrum when frame sum rejection is used. The bottom curve of figure 6 is the difference between the top and middle curves of figure 6.

FIGURE 8: AU Mic spectrum with dark subtracted, corrected for signal loss, and divided by observation time.

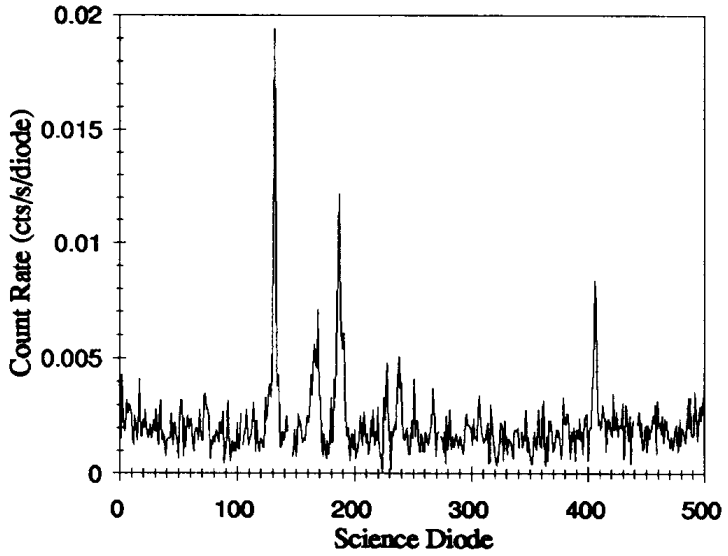

Figure 8 shows the "calibrated" AU Mic data, for FLYLIM=3, with a dark constant subtracted, a correction for signal loss, and division by the observation time. The dark level constant is determined by our S/N code to be 28 percent of the original dark level of 0.0091 counts/sec/diode. The spectrum is then corrected for signal loss, caused by burst noise rejection, by dividing the data by the factor of 0.73, also determined by the S/N code. Note that without this signal correction, object flux is not conserved, when using burst noise rejection.

Acknowledgment

This work is supported by NASA - NAG5-1858.

References

Beaver, E. A., Harms, R. J., and Schmidt, G. W. 1976, Sixth Symposium on Photoelectron Image Devices, in Advances in Electronics and Electron Physics, ed. B. L. Morgan, 40B, 751.

Beaver, E. A., Baity, W. A., Brandt, J. C., Ebbets, D. C., Garner, H., Heap, S. R., Lindler, D. J., Linsky, J. B., Lyons, R. W. and Rosenblatt, E. I. 1991, 10th Symposium on Photoelectronic Image Devices, in Photoelectronic Image Devices, ed. B. L. Morgan, 121, 65.

Maran, S. P., Robinson, R. D., Shore, S. N., Brosius, J. W., Carpenter, K. G., Woodgate, B. E., Linsky, J. L., Brown, A., Byrne, P. B., Kundu, M. R., White, S., Brandt, J. C., Shine, R. A., & Walter, F. M. 1993, Ap. J. [in press].

Press, W. H., Teukolsky, S. A., Vetterling, W. T., Flannery, B. P. 1992, Numerical Recipes in Fortran, Cambridge University Press, 281.

Rosenblatt, E. I., Beaver, E. A., Cohen, R. D., Linsky, J. B., Lyons, R. W. 1991 SPIE Proceedings on Electron Image Tubes and Image Intensifiers II, ed. I. P. Csorba (Bellingham, WA: SPIE) 1449, 72.

Woodgate, B. E., Robinson, R. D., Carpenter, K. G., Maran, S. P., and Shore, S. N. 1992, Ap. J., 397, L95.